

Electron spectroscopy study of the initial stages of iron phthalocyanine growth on highly oriented pyrolytic graphite

Cristina Isvoranu,¹ John Åhlund,^{2,a)} Bin Wang,³ Evren Ataman,¹ Nils Mårtensson,^{2,4} Carla Puglia,² Jesper N. Andersen,¹ Marie-Laure Bocquet,³ and Joachim Schnadt^{1,b)}

¹Department of Physics, Division of Synchrotron Radiation Research, Lund University, Box 118, Lund 221 00, Sweden

²Department of Physics and Materials Science, Uppsala University, Box 530, Uppsala 751 21, Sweden

³Laboratoire de Chimie, Ecole Normale Supérieure de Lyon, 46, Allée d'Italie, 69364 Lyon Cedex 07, France

⁴MAX-Lab, Lund University, Box 118, Lund 221 00, Sweden

(Received 28 August 2009; accepted 17 October 2009; published online 7 December 2009)

The nature of the intermolecular and substrate bonds of iron phthalocyanine adsorbed on highly oriented pyrolytic graphite has been investigated by x-ray photoelectron spectroscopy and x-ray absorption spectroscopy. We find that the molecules grow in a highly ordered fashion with the molecules essentially plane-parallel to the surface in both the mono- and multilayers. The spectra obtained on both types of film are virtually identical, which shows that the bonds both between the adsorbate and substrate and between the molecular layers have a pure van der Waals nature. Supporting density functional theory results indicate that the layers are stabilized by weak hydrogen bonds within the molecular layers. © 2009 American Institute of Physics. [doi:10.1063/1.3259699]

I. INTRODUCTION

Phthalocyanines (cf. Fig. 1 for the chemical structure of iron phthalocyanine, FePc) are among the most important macrocycle molecules, which are characterized by a closed organic framework that holds a central metal atom. Phthalocyanines are widely studied both due to their broad application range (see, e.g., Refs. 1–4) and due to their suitability as a model system for more complicated macrocycles. FePc has been receiving particular interest since its structure and chemistry are very similar to that of the active part of heme (see, e.g., Refs. 1, 5, and 6). Heme is one of the most important biological catalysts, so this similarity suggests that phthalocyanines in general and FePc in particular might be excellent catalyst materials for oxidation and other chemical reactions.^{4,7–11} Indeed, phthalocyanines have, e.g., been employed in the cathodic oxygen dissociation in fuel cells.^{12–23} However, under fuel cell standard conditions, i.e., using pure hydrogen as the feed, the activity of FePc remains below that of the widely used precious metal catalysts such as platinum.^{14,17,18,24} The reason for this remains unclear, since little is known about the catalyst structure during operation and the catalytic mechanism when using the macrocycle catalysts. In general, the functionality and reactivity of macrocycle compounds depend on the atomic-scale geometry and electronic structure of the molecules, both when adsorbed on surfaces and in thin films (see, e.g., Refs. 25–32). Hence it is important to develop a better grasp of the atomic details of the catalytic phase. Our interest here is the investigation of a model system which can enlighten some of these questions. Since the catalytically active material in fuel cells typically is supported by a carbon substrate,³³ we chose

to study the adsorption of FePc on highly oriented pyrolytic graphite (HOPG) by x-ray photoelectron spectroscopy (XPS) and x-ray absorption spectroscopy (XAS). In the following we will show that on HOPG both the mono- and multilayers are characterized by a molecular geometry with the heterocyclic planes parallel to the surface. The same geometry is also found for a three-dimensional (3D) cluster characteristic for the growth of FePc on HOPG.³⁴ The 3D phase can be regarded as a precursor to the monolayer phase, because annealing of this phase leads to the formation of molecular single layer islands. Our results also show that the interactions between the substrate and adsorbate and between the adsorbate layers are weak. Since our experiments could not provide any detailed information on the in-plane intermolecular interactions, we performed density functional theory (DFT) calculations which suggest a stabilization of the molecular networks by weak in-plane hydrogen bonds.

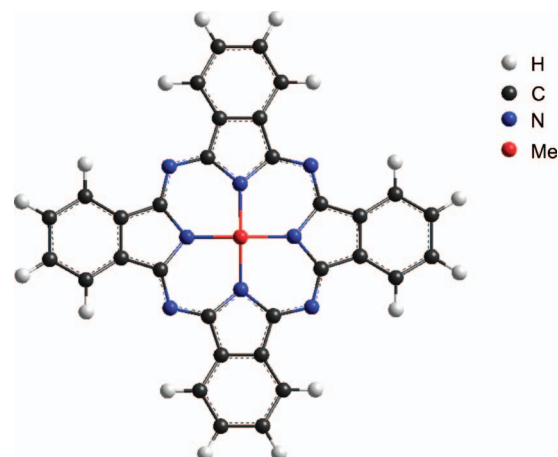


FIG. 1. The molecular structure of FePc.

^{a)}Present address: VG Scienta AB, Box 1520, 750 15 Uppsala, Sweden.

^{b)}Electronic mail: joachim.schnadt@sljus.lu.se.

II. EXPERIMENTAL AND THEORETICAL METHODS

The experiments were performed at beam line I511 (Ref. 35) of the national Swedish synchrotron radiation facility MAX-Laboratory. The surface end station of this beam line consists of two chambers, an analysis chamber with a base pressure of 1×10^{-10} Torr and a preparation chamber with a base pressure which in our experiment was in the high 10^{-10} Torr range. The analysis chamber houses a Scienta R4000 electron energy analyzer, which can be rotated around the beam direction. The beam direction is parallel to the axis of the sample manipulator, and therefore the sample has to be mounted in such a way that its surface inclines by a small angle (ca. 7°) from the beam axis.

The HOPG substrate was freshly cleaved prior to insertion into vacuum. After insertion it was cleaned by flashing to 900°C . FePc, purchased from Sigma-Aldrich, was thermally sublimated onto the sample using a home-built sublimation stage. Prior to deposition, the FePc powder was out-gassed carefully. During evaporation the tantalum crucible holding the FePc was resistively heated to a temperature of around 400°C , while the HOPG substrate was kept at room temperature. The coverage and character of the multilayer films are discussed in more detail below. The monolayer was prepared by heating the multilayer to 400°C for 1 min.^{34,40} Subsequent heating did not lead to any further change in the appearance of the previously obtained spectra. During the measurements the sample was scanned in order to prevent possible beam damage of the FePc molecules.

In the XPS experiments, photon energies of 350, 530, and 130 eV were used for recording the C 1s, N 1s, and valence band photoemission spectra. All spectra were energy calibrated with respect to the C 1s core level of graphite³⁶ at 284.42 eV. The XAS experiments were performed using a number of different geometries, with the electric field vector E parallel and close to normal to the surface, respectively. A small deviation from the normal direction arises from the inclination of the surface with respect to the direction of the incoming light as described above. For the monolayer preparation further XAS scans were performed at angles of 70° , 45° , and 20° between the orientation of the E vector and the surface to determine the molecular inclination with respect to the HOPG surface. The x-ray absorption spectra were divided by the energy-dependent photon flux, which was recorded by measuring the photon-induced current on a gold mesh between the monochromator and sample. After removal of a constant background measured below the first resonance the spectra were then normalized to the intensity of the vacuum level step at about 30 eV above the absorption edge. The photon energy scale of the x-ray absorption spectra was calibrated by recording photoemission spectra excited by first and second order light at relevant photon energies.

All DFT calculations were carried out with the VASP package,³⁷ using ultrasoft pseudopotentials^{38,39} and the Ceperley–Alder version of the local density approximation.^{40,41} The plane-wave basis cutoff was set to 350 eV. The FePc dimer was positioned in a $40 \times 40 \times 10 \text{ \AA}^3$ cuboid supercell. The Brillouin zone was sampled

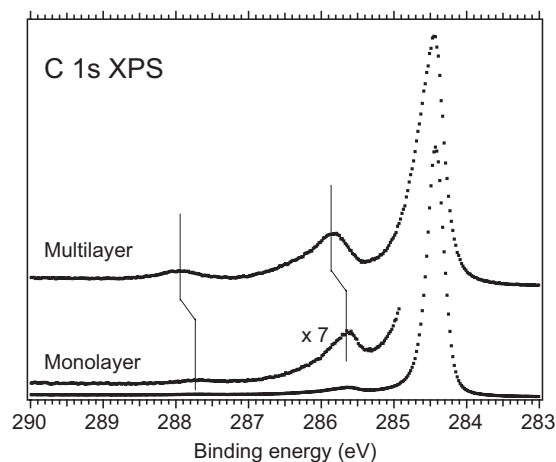


FIG. 2. C 1s x-ray photoemission spectra of the multi- and monolayer preparations of FePc on HOPG. Increasing the coverage from a monolayer to a multilayer leads to a shift to higher binding energies of the molecular features. The overall energy resolution was 90 meV.

with a single k-point at Γ . The Gaussian smearing method with 0.2 eV smearing width was used to accelerate the electronic relaxation. The energy profile presented in Fig. 8 is the result of non-spin-polarized calculations. Spin-polarized calculations were performed for some interaction distances with no effect on the interaction energy values.

III. RESULTS

The C 1s, N 1s, and valence band photoemission spectra are displayed in Figs. 2–5 and the peak positions are reported in Table I. We first turn to the mono- and multilayer C 1s spectra in Fig. 2, with the corresponding least-squares fits in Fig. 3. The spectra consist of several features, which correspond to photoemission from the HOPG substrate (C1), benzene carbon atoms (C2), pyrrole carbon atoms (C3), and shake-up satellites related to photoemission from the benzene (S_{C2}) and pyrrole carbon atoms (S_{C3}). From the feature at around 286 eV binding energy in Fig. 2 (cf. Table I), which is due to photoemission from the pyrrole atoms of FePc,^{42–44} it is seen that the multilayer C 1s spectrum is shifted to higher binding energies as compared to the monolayer C 1s spectrum. The monolayer spectrum is dominated by the graphite peak at 284.42 eV as can be deduced from the fitting results illustrated in Fig. 3(a), while the FePc benzene peak at 284.49 eV gives a small contribution to the main peak only. As stated above, the feature at 285.67 eV binding energy stems from photoemission from the pyrrole carbon atoms of FePc. The intensity ratio of the peaks associated with benzene and pyrrole carbons (considered as the sum of the main peak and shake-up satellite contributions) found in the monolayer spectrum least-squares fits is 3:1 as expected from the stoichiometry of the compound.

The appearance of the C 1s multilayer spectrum agrees well with previous experimental and theoretical work^{45,46} [Fig. 3(b), cf. Table I for binding energies]. The main difference compared to previous work lies in the more asymmetric line shape of the low binding energy peak. The reason for this deviation is the occurrence of the C 1s peak of the graphite substrate, which shows that the investigated

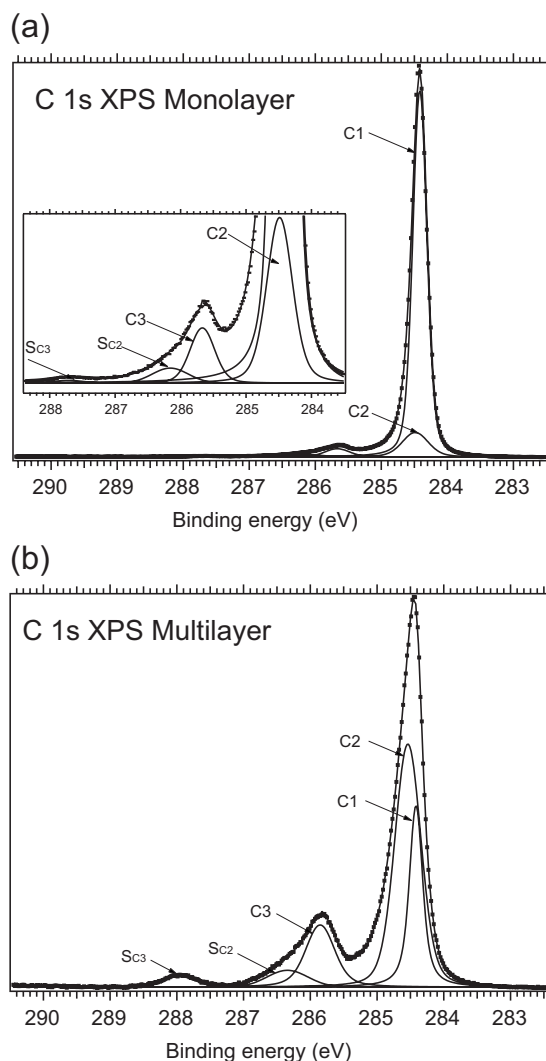


FIG. 3. C 1s x-ray photoemission spectra (experimental data and fit) of the monolayer (a) and multilayer (b) of FePc on HOPG. The solid lines represent the fit and the dotted lines the experimental data. A Shirley-type background was subtracted from the spectra prior to fitting. Five peak components have been fitted to each spectrum. The peaks correspond to the substrate HOPG (C1), the benzene and pyrrole carbon atoms (C2 and C3), and the shake-up satellites associated with the benzene and pyrrole main lines (S_{C2} and S_{C3}). The intensity ratio benzene:pyrrole peaks ($(C2 + S_{C2})/(C3 + S_{C3})$) has been constrained to 3:1, which is the value expected from the stoichiometry of the FePc molecule. The inset in Fig. 3(a) represents a magnified area of part of the monolayer spectrum, for a better view of the fit components.

multilayer is relatively thin. This contribution from the HOPG substrate (C1) was fixed at 284.42 eV and then the main peaks due to photoemission from the molecules were found at 284.54 eV (C2, benzene) and 285.85 eV (C3, pyrrole). The shake-up structures relating to photoemission from benzene (S_{C2}) and pyrrole (S_{C3}) carbons are shifted by 1.8 and 2.1 eV from the corresponding main peaks, respectively. To within the limit of the experiment uncertainty the separation between the main peaks and the satellites is the same for the multilayer and monolayer.

Comparing the mono- and multilayer C 1s spectra, we find a 0.18 eV shift to higher binding energy for the multilayer pyrrole carbon atom photoemission compared to photoemission from the monolayer, while the shift for the

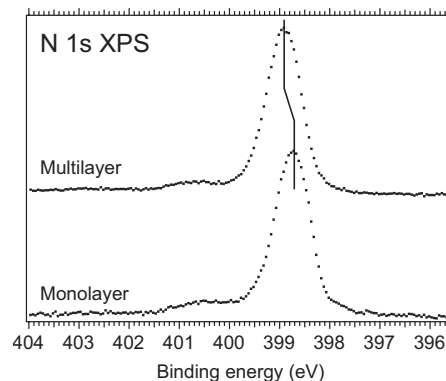


FIG. 4. N 1s x-ray photoemission spectra of the multi- and monolayer preparations of FePc on HOPG measured at an overall energy resolution of 130 meV. The peaks have the same width of 0.78 eV at half maximum.

benzene peak is only 0.05 eV, i.e., of the same order as the measurement uncertainty. For the multilayer the benzene/pyrrole peak intensity ratio ($(C2 + S_{C2})/(C3 + S_{C3})$) is 3.17:1, similar to what we found for the monolayer. The value is also in accordance with previous literature data for thick H_2Pc films (Ref. 41). The analysis of the C 1s core level photoemission peaks shows the same molecular features for both the mono- and multilayer preparations. The only significant difference is the increase in binding energy with coverage (Fig. 2 and Table I), which is seen to be different for the benzene and pyrrole peaks (Table I).

Apart from a shift of approximately 0.17 eV, the N 1s spectra for the monolayer and multilayer preparations in Fig. 4 are virtually identical with main peaks of identical widths (0.78 eV full width at half maximum) and shake-up features at around 1.8 eV above the main peak. The FePc-related features in the mono- and multilayer valence photoemission spectra in Fig. 5 are also in good agreement, as can be seen from a comparison of the monolayer/clean graphite difference and multilayer spectra (however, the difference spectrum fails to correctly reproduce some of the inner valence states at around 20 eV binding energy). The main difference is an overall shift (0.15 eV) which most easily is identified from a comparison of the positions of the highest occupied molecular orbital (HOMO).

In panels (a) and (c) of Fig. 6, the N 1s x-ray absorption spectra are shown for the mono- and multilayer preparations and in panel (b) the corresponding spectra for the 3D cluster

TABLE I. Binding energies in eV for the main photoemission lines, separation between the main line and corresponding shake-up satellite for the C 1s and N 1s photoemission spectra, and HOMO peak position for the mono- and multilayers. The binding energy uncertainty is ± 50 meV.

	Multilayer	Monolayer	$\Delta_{\text{multilayer-monolayer}}$
C 1s benzene (eV)	284.54	284.49	0.05
C 1s pyrrole (eV)	285.85	285.67	0.18
$\Delta_{\text{benzene-pyrrole}}$ (eV)	1.31	1.18	
$\Delta_{\text{benzene-satellite}}$ (eV)	1.8	1.8	
$\Delta_{\text{pyrrole-satellite}}$ (eV)	2.1	2.05	
N 1s main line (eV)	398.90	398.73	0.17
$\Delta_{\text{N 1s-satellite}}$ (eV)	1.82	1.79	
HOMO (eV)	1.79	1.64	0.15

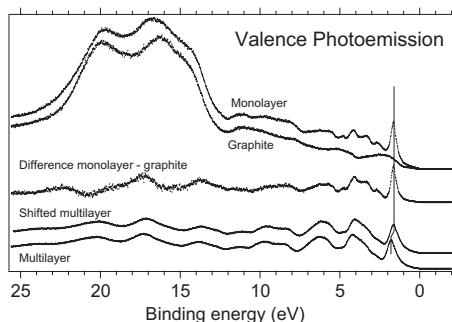


FIG. 5. Valence photoemission spectra of the indicated preparations. The middle spectrum is the difference of the monolayer (top) and the clean graphite (second topmost) spectrum. This difference spectrum is compared to the multilayer spectrum below, which has been shifted by -0.15 eV in order to align the HOMO features. All spectra were measured at 55° from normal emission. In this geometry it is possible to resolve both the σ and π states of the molecule (Ref. 45). The overall instrumental resolution was 60 meV for the monolayer and multilayer spectra and 30 meV for the graphite spectrum.

growth at low coverage mentioned in the Sec. I. The resonances in the N $1s$ x-ray absorption spectra represent the unoccupied molecular orbitals with at least partial p -character and weight on the nitrogen atom. For all preparations the spectra show strong intensity due to the lowest π^* resonances of FePc when the sample is irradiated with the x-ray E -vector perpendicular to the surface. In contrast, for irradiation with the E -vector parallel to the surface the intensity of these resonances vanishes nearly completely. This observation expresses clearly that FePc grows on HOPG in a flat geometry, and this is valid not only for the first monolayer, but also for subsequent layers as well as the molecules in the 3D cluster growth.

In order to render this statement more quantitative we measured monolayer N $1s$ x-ray absorption at further incidence angles. Figure 7 shows the peak height of the lowest unoccupied molecular orbital (LUMO) of the monolayer as a function of the angle between the electric field vector and the surface.^{47,48} The angle dependence reveals that the π^* orbitals are oriented perpendicular to the surface ($\pm 1.7^\circ$), which proves that the monolayer molecules lie essentially perfectly flat on the HOPG surface. These data agree well with STM studies of the first layer growth of FePc on HOPG,³⁴ which also showed a flat-lying geometry of the adsorbates. We expect exactly the same tilt angle for the multilayer and 3D clusters, since their x-ray absorption spectra at grazing and normal incidence angles of the E -vector relative to the surface exhibit exactly the same behavior.

In Fig. 8 the results of a DFT calculation for the molecule-molecule interaction are shown. The potential curve for a FePc dimer in the gas phase is characterized by a minimum for an intermolecular distance close to 3.1 Å and, hence, the dimer is stabilized with respect to the separated molecules by a small energy gain of approximately 0.2 eV. As will be discussed below, this energy gain is attributed primarily to the formation of weak hydrogen bonds between the bridging nitrogen atoms on one molecule and the benzene hydrogen atoms on the neighbor molecules. It is noted

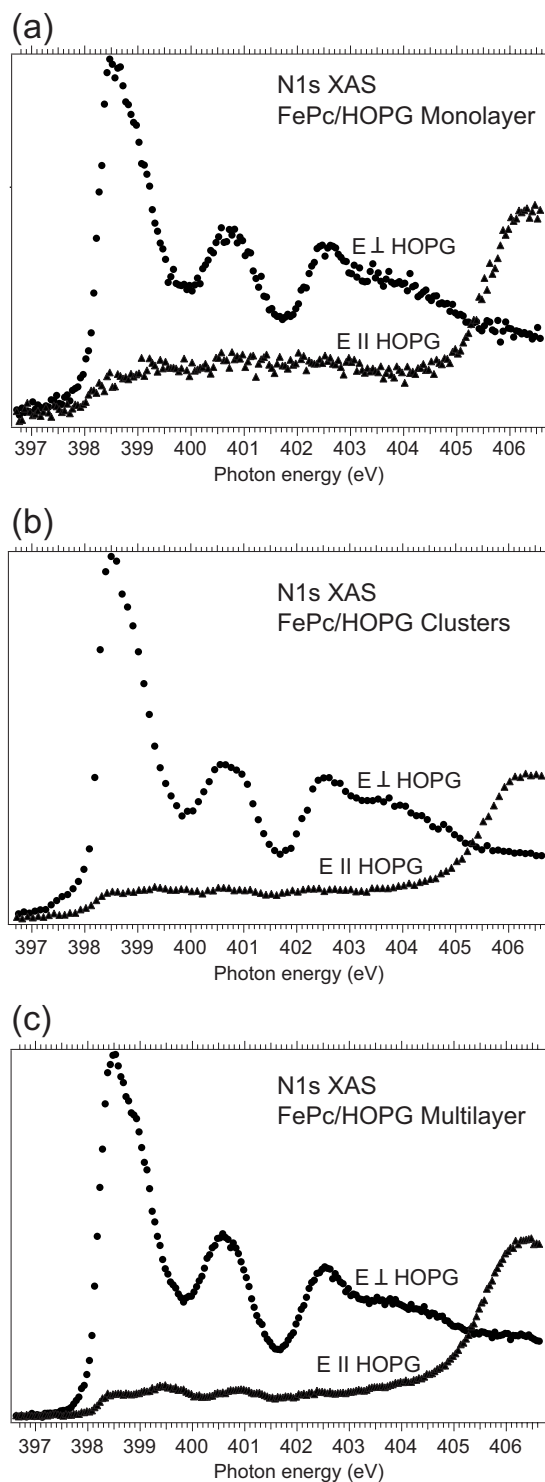


FIG. 6. N $1s$ x-ray absorption spectra of FePc monolayers (a), 3D clusters (b), and multilayers (c) on HOPG. The measurements were carried out in Auger yield at a photon energy resolution of around 60 meV for the spectra in panels (a) and (b) and 90 meV for the spectra in (c).

that the distances of the optimized geometry fit well with the STM data of FePc/HOPG measured by Åhlund *et al.* (Ref. 34).

IV. DISCUSSION

There are a couple of issues that we would like to discuss in more detail. In particular, we will show that FePc

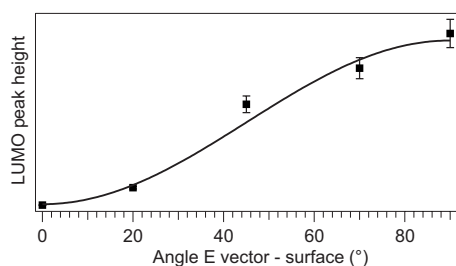


FIG. 7. LUMO resonance intensity for the monolayer preparation as a function of the angle between the electric field and the surface. The degree of in-plane polarization of the light is 97%. The fit resulted in a 90 degree tilt angle for the π^* resonance with respect to the surface, which indicates that the molecules are flat on the HOPG surface.

binds only weakly to the graphite surface in a flat-lying geometry and that the electronic structure of FePc is at most only weakly perturbed by the bond to the substrate. The intermolecular bond is also weak and we propose that the in-plane bond is characterized by weak hydrogen bonds, while the interlayer bonds are proposed to have a pure van der Waals nature.

Before going into any detail of the bonding, we would like to clarify the nature of the investigated multilayer. The multilayer C 1s photoemission spectrum in Fig. 3 contains a significant contribution from the substrate C 1s peak, which implies that the organic film was relatively thin. We can make a crude estimation for the film thickness from a comparison of the absolute intensities of the N 1s peaks for the two preparations measured using the same beam line and analyzer settings. The comparison shows an N 1s intensity that is approximately six times higher for the multilayer as compared to the monolayer. This implies that the multilayer must be more than six layers thick, since the peak ratio will underestimate the multilayer intensity due to electron scattering. However, the estimation is complicated by the finding that FePc grows in a Volmer–Weber mode, i.e., in 3D clusters.³⁴ Hence, the multilayer thickness is expected to be inhomogeneous and even at very large nominal coverages there might exist parts of the surface which either are bare or covered by very thin molecular layers only. The observation of the substrate C 1s signal in the multilayer C 1s spectrum and of the onset of states evident in the valence band spectra (Figs. 3 and 5) might be related to such domains of low FePc coverages or bare surface, while, at the same time, many of the multilayer islands might be characterized by very large

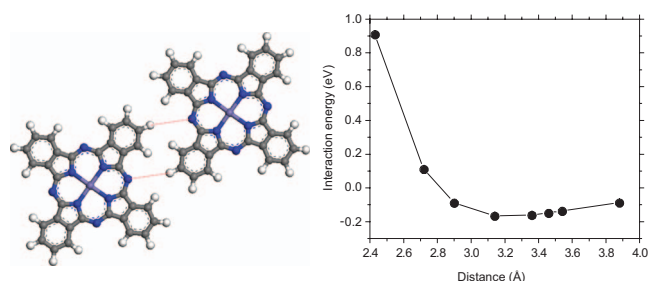


FIG. 8. Interaction energy between two FePc molecules as a function of the intermolecular distance (red lines between the molecules). The result indicates that the optimum distance is very close to 3.1 Å at an interaction energy of -0.17 eV.

thicknesses. The multilayer photoemission spectrum contains then information from both high coverage and low coverage domains on the surface. For this reason, we are only able to provide the lowest limit for the surface coverage, which is six monolayers.

As already stated above, the XPS results for the mono- and multilayers (Figs. 2–5) are very similar in terms of peak shapes, peak widths, and binding energy separation between the main peak and the corresponding shake-up satellite. The only notable difference is that the photoemission features are shifted to higher binding energies when going from the monolayer to the multilayer coverage (cf. Table I). We suggest that this shift is related to a better core-hole screening provided by the graphite substrate compared to the screening ability of the FePc multilayer. In a previous study of nickel phthalocyanines on HOPG (Ref. 43) in a similar coverage range such a shift was not observed. We attribute this difference to the better overall resolution in our experiments.

The difference in intensity ratio between the benzene and pyrrole C 1s peaks for multilayer and monolayer—3.17:1 for the multilayer and 3:1 for the monolayer—could be due to photoelectron diffraction in the multilayer. Such processes could lead to intensity changes in the photoemission peaks, thus affecting the final intensity ratio. Also, the presence of the HOPG peak could to some extent affect the intensity ratio.

We observe different binding energy shifts between the multi- and monolayer for the benzene carbon atoms (0.05 eV) and the pyrrole carbons (0.18 eV). The N 1s shift is 0.17 eV, similar to that of the C 1s pyrrole peak. Since the electronic structure otherwise is unchanged between the multilayer and monolayer, we interpret these shifts in terms of an improved pyrrole carbon core-hole screening provided by the HOPG substrate as opposed to that provided to the benzene carbon core holes. This indicates that the pyrrole rings are slightly closer to the HOPG surface than the benzene. In principle, the screening could occur via a charge transfer process upon ionization; however, since the electronic coupling between the adsorbate and substrate is very weak, the time scale of charge transfer screening is expected to be too long for the process to be relevant for the observed chemical shifts.⁴⁹ Instead we assume that the final state of the XPS measurements is characterized by pure image-charge screening. While the relatively small singularity index α of HOPG^{36,50} indicates that graphite does not fully comply with an entirely metallic behavior, the in-plane mobility of the electrons in the graphite layers should be large enough for the build-up of a complete image charge. We explain the difference in binding energy shift between the monolayer and multilayer benzene and pyrrole C 1s peaks (0.05 eV as opposed to 0.18 eV, i.e., a difference of 0.13 eV) in terms of a difference in screening energy. This difference is given by the difference in Coulomb energy between the core hole/image charge pairs for the pyrrole and benzene carbon atoms. More specifically, $\Delta E = -(e^2/4\pi\epsilon_0)((1/r_{\text{benzene}}) - (1/r_{\text{pyrrole}}))$, where e represents the electron charge, ϵ_0 is the vacuum permittivity, and r_{benzene} and r_{pyrrole} represent the distances between the benzene and pyrrole core-holes and the image charges. Assuming that the distance between the

pyrrole core-hole and its image charge is approximately 6.7–6.8 Å, which corresponds to twice the interlayer distance in graphite and, likewise, to the interlayer distance in bulk FePc, one obtains a difference in height of the benzene and pyrrole atoms over the surface of around 0.2 Å. Such a height difference results in an insignificant angular change in the orientation of the molecular lobes, which is not expected to be resolved by the STM or the XAS experiments.

The HOMO shift (0.15 eV), intermediate between the pyrrole and benzene C 1s shift, is consistent with this hypothesis. The experimental HOMO feature, which is a combination of different orbitals,^{51,52} is delocalized over the entire macrocycle. This makes the HOMO contain contributions from both inequivalent carbon atoms and most likely from nitrogen, as well, and it is then expected to exhibit an intermediate screening behavior as compared to that of the pyrrole and benzene carbons.

One main aspect brought out by the XPS experiments is thus the very close similarity of the N 1s and C 1s mono- and multilayer spectra, which leads us to suggest that the chemical and electronic structure of the FePc in the mono- and multilayers is essentially the same. The argument is further supported by the behavior of valence band spectra (Fig. 5). The difference spectrum monolayer/clean graphite shows the same features as the multilayer spectrum. In consequence, the difference monolayer/clean graphite is a good estimate for the valence molecular features of the monolayer decoupled from the substrate. This shows that the molecular orbitals of FePc are at most weakly affected by the adsorption process which once again supports the idea of a very weak molecule-substrate interaction. A similarly weak interaction has been observed for H₂Pc on graphite,⁵³ which, however, is different from the present system in that these molecules do not possess any reactive metal center.

Turning to the XAS experiments (Figs. 6 and 7), our results show that monolayers, multilayers, and 3D clusters of FePc on HOPG lie flat on the surface. For monolayers of phthalocyanines, previous studies report adsorption geometries with the molecular plane parallel to the surface in almost all cases, with the exception of the polycrystalline substrates and Si(100) (see, e.g., Refs. 44 and 54–61). On Si(111), Si(001), and indium tin oxide,^{45,59,62,63} on rough or polycrystalline substrates,^{54,64} as well as on strongly interacting substrates such as Al(100), Ni₃Al(111) (Refs. 65 and 66) multilayers of phthalocyanines are known to adopt a standing geometry. On metallic substrates such as Ag(111), Au(110), and Au(001), the multilayers are flat at room temperature.^{60,64,67} For weakly interacting substrates, such as HOPG which is our main interest, there is a consensus in literature that monolayers and thin layers of FePc grow in a flat-lying geometry.^{43,67,68} For the multilayer case, data obtained from high resolution electron energy loss spectroscopy⁶⁷ support the idea of a flat geometry for very large molecular coverages, while AFM, VB photoemission spectroscopy, and metastable-atom electron spectroscopy data^{43,66} suggest a standing-up geometry at high coverages of phthalocyanines on HOPG. As discussed above, we cannot provide an exact FePc surface coverage, since the multilayers grow in a Volmer–Weber mode. This implies that we

cannot finally decide whether truly thick films of FePc on HOPG grow in a flat-lying or standing-up mode. However, in all cases investigated here, we find a flat geometry. It is worthwhile to once again point out that parts of the surface might have been covered with films of a sizeable thickness.

We note that the x-ray absorption spectra in Fig. 6 are essentially identical for all three preparations, which is in line with our hypothesis of a great similarity of the electronic structures of the mono- and multilayer preparations. The overall great similarity of the mono- and multilayer x-ray photoemission and x-ray absorption spectra strongly favors the idea that the growth of FePc on HOPG relies on weak substrate/adsorbate and intermolecular forces, i.e., van der Waals forces, which do not change the chemical and electronic state of the molecules. This argument holds primarily for the adsorbate/substrate and out-of-plane molecular interactions. The monolayer, however, is characterized by the adsorbate/substrate and in-plane intermolecular interactions, since FePc adsorbs in a flat geometry on HOPG. Previous STM work³⁴ has shown that the FePc monolayer molecular chains on HOPG are oriented with one of the benzene rings of one molecule toward the bridging nitrogen of the neighbor molecule. In such an orientation weak C–H···N hydrogen bond formation may occur.⁶⁹ It is not straightforward to distinguish between van der Waals and weak hydrogen bonding interactions, since they have similar strengths.⁶⁶ Theory can contribute to enlighten this difference. Since van der Waals interactions are not properly taken into account by the pure DFT calculations,^{70–72} the presence of the minimum in Fig. 8 implies the formation of a weak hydrogen bond between the benzene C–H group on one molecule and the lone pair orbital of one of the bridging nitrogen atoms on the adjacent molecule. The combined results of our experiments and DFT calculations indicate that the in-plane molecule-molecule interaction is most likely characterized by a weak hydrogen bond formation.

V. CONCLUSIONS

X-ray photoemission and x-ray absorption spectroscopy have been used to characterize monolayers and thin multilayers of iron phthalocyanine grown on HOPG. The measurements show a large degree of ordering in the growth and a flat adsorbate geometry in both the mono- and multilayers. There is only a slight bending of the molecule for the monolayer as indicated by the benzene and pyrrole C 1s binding energies. The similarity between the x-ray photoemission and x-ray absorption spectra for the mono- and multilayers suggests that the films are characterized by weak substrate/adsorbate and out-of-plane intermolecular interactions (van der Waals interactions). More than that, the different types of films have very similar chemical and electronic structures. For the in-plane molecule-molecule interaction, the DFT calculations suggest a weak hydrogen bond formation.

ACKNOWLEDGMENTS

We would like to thank the staff of MAX-laboratory for technical support. The European Commission is acknowledged for financial support through the MONET Early Stage

Researcher Training Network Grant No. MEST-CT-2005-020908. Furthermore, we would like to thank Vetenskapsrådet (VR) for funding.

- ¹L. R. Milgrom, *The Colours of Life: An Introduction to the Chemistry of Porphyrins and Related Compounds* (Oxford University Press, Oxford, 1997).
- ²L. Valli, *Adv. Colloid Interface Sci.* **116**, 13 (2005).
- ³P. R. Somani and S. Radhakrishnan, *Mater. Chem. Phys.* **77**, 117 (2003).
- ⁴O. L. Kaliya, E. A. Lukyanets, and G. N. Vorozhtsov, *J. Porphy. Phthalocyanines* **3**, 592 (1999).
- ⁵H. R. Horton, L. A. Moran, R. S. Ochs, J. D. Rawn, and K. G. Scrimgeour, *Principles of Biochemistry*, 2nd ed. (Prentice Hall, New Jersey, 1996).
- ⁶C. K. Mathews, K. E. van Holde, and K. G. Ahern, *Biochemistry*, 3rd ed. (Addison Wesley Longman, San Francisco, 2000).
- ⁷M. Toledo, A. M. S. Lucko, and Y. Gushikem, *J. Mater. Sci. Lett.* **39**, 6851 (2004).
- ⁸J. C. Obirai and T. Nyokong, *J. Electroanal. Chem.* **600**, 251 (2007).
- ⁹M. I. Newton, T. K. H. Starke, M. R. Willis, and G. McHale, *Sens. Actuators B* **67**, 307 (2000).
- ¹⁰Y. Lu and R. G. Reddy, *Int. J. Hydrogen Energy* **33**, 3930 (2008).
- ¹¹J. R. Darwent, P. Douglas, A. Harriman, G. Porter, and M. C. Richoux, *Coord. Chem. Rev.* **44**, 83 (1982).
- ¹²K. Wiesener, D. Ohms, V. Neumann, and R. Franke, *Mater. Chem. Phys.* **22**, 457 (1989).
- ¹³M. Lefèvre, J. P. Dodelet, and P. Bertrand, *J. Phys. Chem. B* **106**, 8705 (2002).
- ¹⁴M. Lefèvre, J. P. Dodelet, and P. Bertrand, *J. Phys. Chem. B* **104**, 11238 (2000).
- ¹⁵F. C. Anson, C. Shi, and B. Steiger, *Acc. Chem. Res.* **30**, 437 (1997).
- ¹⁶J. Ma, J. Wang, and Y. Liu, *J. Power Sources* **172**, 220 (2007).
- ¹⁷H. Schulenburg, S. Stankov, V. Schünemann, J. Radnik, I. Dorbandt, S. Fiechter, P. Bogdanoff, and H. Tributsch, *J. Phys. Chem. B* **107**, 9034 (2003).
- ¹⁸L. Zhang, J. Zhang, D. P. Wilkinson, and H. Wang, *J. Power Sources* **156**, 171 (2006).
- ¹⁹F. Zhao, F. Harnisch, U. Schröder, F. Scholz, P. Bogdanoff, and I. Herrmann, *Electrochem. Commun.* **7**, 1405 (2005).
- ²⁰L. Zhang, C. Song, J. Zhang, H. Wang, and D. P. Wilkinson, *J. Electrochem. Soc.* **152**, A2421 (2005).
- ²¹K. Arihara, L. Mao, P. A. Liddell, E. Marino-Ochoa, A. L. Moore, T. Imase, D. Zhang, T. Sotomura, and T. Ohsaka, *J. Electrochem. Soc.* **151**, A2047 (2004).
- ²²H. Jahnke, M. Schönborn, and G. Zimmermann, *Top. Curr. Chem.* **61**, 133 (1976).
- ²³R. Jasinski, *J. Electrochem. Soc.* **112**, 526 (1965).
- ²⁴S. Baranton, C. Coutanceau, E. Garnier, and J.-M. Léger, *J. Electroanal. Chem.* **590**, 100 (2006).
- ²⁵S. Berner, S. Biela, G. Ledung, A. Gogoll, J.-E. Bäckvall, C. Puglia, and S. Oscarsson, *J. Catal.* **244**, 86 (2006).
- ²⁶S. Srinivasan and W. T. Ford, *J. Mol. Catal.* **64**, 291 (1991).
- ²⁷H. Grennberg, A. Gogoll, and J. E. Bäckvall, *J. Org. Chem.* **56**, 5808 (1991).
- ²⁸C. Ercolani, F. Monacelli, and G. Rossi, *Inorg. Chem.* **18**, 712 (1979).
- ²⁹C. Ercolani, G. Rossi, and F. Monacelli, *Inorg. Chim. Acta* **44**, L215 (1980).
- ³⁰C. Ercolani, M. Gardini, F. Monacelli, G. Pennesi, and G. Rossi, *Inorg. Chem.* **22**, 2584 (1983).
- ³¹H. Grennberg and J. E. Bäckvall, *Acta Chem. Scand.* **47**, 506 (1993).
- ³²K. Morishige, S. Tomoyasu, and G. Iwano, *Langmuir* **13**, 5184 (1997).
- ³³L. Carrette, K. A. Friedrich, and U. Stimming, *Fuel Cells* **1**, 5 (2001).
- ³⁴J. Åhlund, J. Schnadt, K. Nilson, E. Göthelid, J. Schiessling, F. Besenbacher, N. Mårtensson, and C. Puglia, *Surf. Sci.* **601**, 3661 (2007).
- ³⁵R. Denecke, P. Väterlein, M. Bässler, N. Wassdahl, S. Butorin, A. Nilsson, J.-E. Rubensson, J. Nordgren, N. Mårtensson, and R. Nyholm, *J. Electron Spectrosc. Relat. Phenom.* **101–103**, 971 (1999).
- ³⁶T. Balasubramanian, J. N. Andersen, and L. Wallden, *Phys. Rev. B* **64**, 205420 (2001).
- ³⁷G. Kresse and J. Furthmüller, *Phys. Rev. B* **54**, 11169 (1996).
- ³⁸D. Vanderbilt, *Phys. Rev. B* **41**, 7892 (1990).
- ³⁹G. Kresse and J. Hafner, *J. Phys.: Condens. Matter* **6**, 8245 (1994).
- ⁴⁰D. M. Ceperley and B. J. Alder, *Phys. Rev. Lett.* **45**, 566 (1980).
- ⁴¹J. P. Perdew and A. Zunger, *Phys. Rev. B* **23**, 5048 (1981).
- ⁴²Y. Niwa, H. Kobayashi, and T. Tsuchiya, *J. Chem. Phys.* **60**, 799 (1974).
- ⁴³L. Ottaviano, S. Di Nardo, L. Lozzi, M. Passacantando, P. Picozzi, and S. Santucci, *Surf. Sci.* **373**, 318 (1997).
- ⁴⁴N. Papageorgiou, E. Salomon, T. Angot, J.-M. Layet, L. Giovanelli, and G. Le Lay, *Prog. Surf. Sci.* **77**, 139 (2004).
- ⁴⁵J. Åhlund, K. Nilson, J. Schiessling, L. Kjeldgaard, S. Berner, N. Mårtensson, C. Puglia, B. Brena, M. Nyberg, and Y. Luo, *J. Chem. Phys.* **125**, 034709 (2006).
- ⁴⁶B. Brena, Y. Luo, M. Nyberg, S. Carniato, K. Nilson, Y. Alfredsson, J. Åhlund, N. Mårtensson, H. Siegbahn, and C. Puglia, *Phys. Rev. B* **70**, 195214 (2004).
- ⁴⁷J. Stöhr and D. A. Outka, *Phys. Rev. B* **36**, 7891 (1987).
- ⁴⁸J. Stöhr, *NEXAFS Spectroscopy* (Springer, Berlin, 1992).
- ⁴⁹O. Björneholm, A. Nilsson, A. Sandell, B. Hernnäs, and N. Mårtensson, *Phys. Rev. Lett.* **68**, 1892 (1992).
- ⁵⁰M. R. C. Hunt, *Phys. Rev. B* **78**, 153408 (2008).
- ⁵¹M. S. Liao and S. Scheiner, *J. Chem. Phys.* **114**, 9780 (2001).
- ⁵²N. Marom and L. Kronik, *Appl. Phys. A: Mater. Sci. Process.* **95**, 165 (2009).
- ⁵³K. Nilson, J. Åhlund, B. Brena, E. Göthelid, J. Schiessling, N. Mårtensson, and C. Puglia, *J. Chem. Phys.* **127**, 114702 (2007).
- ⁵⁴E. Salomon, N. Papageorgiou, T. Angot, A. Verdini, A. Cossaro, L. Floreano, A. Morgante, L. Giovanelli, and G. Le Lay, *J. Phys. Chem. C* **111**, 12467 (2007).
- ⁵⁵X. Lu and K. W. Hipps, *J. Phys. Chem. B* **101**, 5391 (1997).
- ⁵⁶C. Ludwig, R. Strohmaier, J. Petersen, B. Gompf, and W. Eisenmenger, *J. Vac. Sci. Technol. B* **12**, 1963 (1994).
- ⁵⁷R. Strohmaier, C. Ludwig, J. Petersen, B. Gompf, and W. Eisenmenger, *J. Vac. Sci. Technol. B* **14**, 1079 (1996).
- ⁵⁸G. Dufour, C. Poncey, F. Rochet, H. Roulet, M. Sacchi, M. De Santis, and M. De Crescenzi, *Surf. Sci.* **319**, 251 (1994).
- ⁵⁹T. S. Ellis, K. T. Park, S. L. Hulbert, M. D. Ulrich, and J. E. Rowe, *J. Appl. Phys.* **95**, 982 (2004).
- ⁶⁰Z. H. Cheng, L. Gao, Z. T. Deng, Q. Liu, N. Jiang, X. Lin, X. B. He, S. X. Du, and H.-J. Gao, *J. Phys. Chem. C* **111**, 2656 (2007).
- ⁶¹M. Takada and H. Tada, *Chem. Phys. Lett.* **392**, 265 (2004).
- ⁶²C. Dufour, C. Poncey, F. Rochet, H. Roulet, S. Iacobucci, M. Sacchi, F. Yubero, N. Motta, M. N. Piancastelli, A. Sgarlata, and M. De Crescenzi, *J. Electron Spectrosc. Relat. Phenom.* **76**, 219 (1995).
- ⁶³H. Peisert, T. Schwieger, J. M. Auerhammer, M. Knupfer, M. S. Golden, J. Fink, P. R. Bressler, and M. Mast, *J. Appl. Phys.* **90**, 466 (2001).
- ⁶⁴I. Biswas, H. Peisert, M. Nagel, M. B. Casu, S. Schuppler, P. Nagel, E. Pellegrin, and T. Chassé, *J. Chem. Phys.* **126**, 174704 (2007).
- ⁶⁵A. Ruocco, F. Evangelista, R. Gotter, A. Attili, and G. Stefani, *J. Phys. Chem. C* **112**, 2016 (2008).
- ⁶⁶S. Kera, M. B. Casu, K. R. Bauchspieß, D. Batchelor, T. Schmidt, and E. Umbach, *Surf. Sci.* **600**, 1077 (2006).
- ⁶⁷H. Yamane, Y. Yabuuchi, H. Fukagawa, S. Kera, K. K. Okudaira, and N. Ueno, *J. Appl. Phys.* **99**, 093705 (2006).
- ⁶⁸S. D. Wang, X. Dong, C. S. Lee, and S. T. Lee, *J. Phys. Chem. B* **108**, 1529 (2004).
- ⁶⁹S. J. Grabowski, *Hydrogen Bonding: New Insights, Challenges and Advances in Computational Chemistry and Physics*. Vol. 3 (Springer, Dordrecht, 2006).
- ⁷⁰J. Schnadt, E. Rauls, W. Xu, R. T. Vang, J. Knudsen, E. Lægsgaard, Z. Li, B. Hammer, and F. Besenbacher, *Phys. Rev. Lett.* **100**, 046103 (2008).
- ⁷¹A. Bilic, J. R. Reimers, N. S. Hush, R. C. Hoft, and M. J. Ford, *J. Chem. Theory Comput.* **2**, 1093 (2006).
- ⁷²P. S. Bagus, K. Hermann, and C. Wöll, *J. Chem. Phys.* **123**, 184109 (2005).